Scientific Research Publishing

Advances in Bioscience and Biotechnology, 2024, 15, 443-461
https://www.scirp.org/journal/abb
ISSN Online: 2156-8502
ISSN Print: 2156-8456

A Novel and Functional Artificial Bruch's Membrane Made of Poly (ε-Caprolactone)/Gelatin for Retinal Pigment Epithelium Restoration

López Edith[1], Silva-Bermudez Phaedra[2], Gonzalez-Salinas Roberto[3], Velasquillo Cristina[4], Torres-Romero Abigail[3], López-Colomé Ana María[1], Pérez Armando[5], Gina Prado-Prone[2], Edgar Ramos-Martínez[6], Iván Ramos-Martínez[7], Quiroz-Mercado Hugo[3], Hernández-Zimbrón Luis Fernando[8,9*]

[1]Instituto de Fisiología Celular, Universidad Nacional Autónoma de México, Ciudad de México City, México
[2]Unidad de Ingeniería de Tejidos, Terapia Celular y Medicina Regenerativa; Instituto Nacional de Rehabilitación Luis Guillermo Ibarra Ibarra, Ciudad de México, México
[3]Departamento de Investigación, Asociación Para Evitar la Ceguera, Ciudad de México, México
[4]Subdirección de Investigación Tecnológica, Instituto Nacional de Rehabilitación Luis Guillermo Ibarra Ibarra, Ciudad de México, México
[5]Departamento de Biología Celular y Tisular, Facultad de Medicina, Universidad Nacional Autónoma de México, Ciudad de México, México
[6]Escuela de Ciencias, Universidad Autónoma Benito Juárez de Oaxaca, Oaxaca, México
[7]Departamento de Medicina y Zootecnia de Cerdos, Facultad de Medicina Veterinaria y Zootecnia, Universidad Nacional utónoma de México, México
[8]Laboratorio de Investigación Interdisciplinaria, Área de Optometría, Escuela Nacional de Estudios Superiores Unidad León, Universidad Nacional Autónoma de México, León Guanajuato, México
[9]Laboratorio Nacional de Óptica de la Visión-Centro de Investigaciones en Óptica, León Guanajuato, México
Email: *lhernandez@enes.unam.mx

How to cite this paper: Edith, L., Phaedra, S.-B., Roberto, G.-S., Cristina, V., Abigail, T.R., María, L.-C.A., Armando, P., Prado-Prone, G., Ramos-Martínez, E., Ramos-Martínez, I., Hugo, Q.-M. and Fernando, H.-Z.L. (2024) A Novel and Functional Artificial Bruch's Membrane Made of Poly (ε-Caprolactone)/Gelatin for Retinal Pigment Epithelium Restoration. *Advances in Bioscience and Biotechnology*, **15**, 443-461.
https://doi.org/10.4236/abb.2024.158027

Received: March 23, 2024
Accepted: August 12, 2024
Published: August 15, 2024

Abstract

Purpose: The primary aim of this paper is to design, create, and improve functional and artificial Bruch's membranes (BM) using bioengineering techniques, which can be applied in the treatment of maculopathies by supporting the growth and maintenance of retinal pigment epithelium (RPE) cells, thereby potentially enabling subretinal implantation in patients. **Methods**: We fabricated by electrospinning ultrathin 3D nanofibrous membranes from Polycaprolactone (PCL), and different concentrations of gelatin (5%, 15% and 30%). ARPE-19 cells were seeded onto these artificial membranes. MTT assays were performed in order to evaluate ARPE-19 cell viability and cytotoxicity. IF assays were realized to observe the ARPE-19 cells onto each membrane. Ultrastructure of the modified Bruch's membrane and ARPE-19 morphology after 25 days of

culture were studied with transmission and scanning electron microscopy. To evaluate expression changes in markers of ARPE-19 (RPE65 and ZO-1) qRT-PCR assays were realized. Data from three independent experiments were pooled and expressed as the mean SD. A confidence level of P 0.05 was considered to be statistically significant. **Results** ARPE-19 cells grew on PCL/Gelatin membranes mainly in PCL/30% gelatin combination, which had not cytotoxic effect. RPE65/cytokeratin-18/ and actin-positive ARPE-19 cells formed a correctly orientated monolayer of polygonal cells with morphological polarity. The apical cell surfaces exhibited abundant protruding microfolds. Moreover, zones of polygonal border look as if ARPE-19 cells fused among, suggesting the presence of tight junctions. The expression of RPE65 and ZO-1 was unchanged. **Conclusion**s: PCL/30% Gelatine membranes may imitate the natural BM to such extent that they support RPE-cells and exhibited RPE-like morphology. The engineering of a human RPE monolayer with these artificial BM, emulating the *in vivo* retina, arouse their potential subretinal implantation in patients with wet age-related macular degeneration (AMD) where there is a rupture of the Bruch's membrane.

Keywords

Artificial Bruch's Membrane, Electrospinning, ARPE-19 Cells, Age-Related Macular Degeneration

1. Introduction

This Bruch's membrane (BM) is an ultrathin, acellular, five-layered extracellular matrix (ECM), separates the retinal pigment epithelium (RPE) from the choriocapillary lamina of the choroid and supports RPE cells and the choriocapillary endothelial cells. This special ECM undergoes significant age-related changes involved in age related macular degeneration (AMD) and other chorioretinal diseases [1]-[3].

AMD is a well-characterized disease, recognized as the leading cause of visual impairment in individuals over 60 years old. Early AMD is characterized by drusen formation, macular pigmentary changes, and mild to moderate vision loss [3]. The "dry" or atrophic form of AMD is the most common, featuring progressive RPE dysfunction, photoreceptor loss, and retinal degeneration. The less common "wet" form, responsible for 90% of severe vision loss due to AMD, involves choroidal neovascularization (CNV) with intraretinal or subretinal leakage, hemorrhage, and RPE detachments [4] [5]. Persistent exudation from the subretinal fibrovascular compartment leads to fibrovascular scar formation, disrupting the integrity between choriocapillaris, RPE, and photoreceptors, ultimately causing central vision loss [3].

RPE cells, crucially involved in maintaining retinal homeostasis, are polarized with well-developed junctional complexes. They feature basal domains with numerous mitochondria-invaginations, apical domains surrounding photoreceptor

outer segments, and specialized organelles such as melanin granules, lysosomes, and smooth endoplasmic reticulum. Functions include forming the blood-retina barrier, absorbing light, phagocytosing shed rod and cone components, and recycling retinoids essential for photoreceptor function and survival [6]. Alterations in RPE function play a pivotal role in the pathogenesis of retinal diseases such as retinitis pigmentosa and AMD [6] [7].

Pathophysiological changes in BM during wet AMD compromise normal RPE functions. Structural alterations in BM's constituent proteins, which normally provide a barrier for choroidal vessels, disrupt the regulated transfer of water, solutes, and macromolecules between RPE and choroid, crucial for RPE support [6]. Restoring BM's structural integrity holds promise as a therapy for wet AMD.

Current treatments for wet AMD, including antiangiogenic drugs, photodynamic therapy, and laser photocoagulation, do not restore BM's structure or function, particularly in advanced cases [3]. A basal membrane capable of supporting transplanted cell viability and nourishment is thus essential [3]. Efforts have focused on developing BM substitutes that facilitate functional RPE monolayer delivery [6] [8].

Artificial BMs for RPE transplantation have been developed using biocompatible, biodegradable biomaterials such as modified human amniotic membrane, collagen, fibrin, and various synthetic polymers (e.g., poly (epsilon-caprolactone) [PCL], poly (L-lactide-co-glycolide) [PLGA], poly (L-lactide-co-D, L-lactide) [PLDLA], poly (L-lactide) [PLLA]), silk fibroin-chitosan, and chitosan-gelatin as carriers [6] [8]-[11]. However, some scaffolds fail to preserve native BM's structural features and fail to induce and maintain RPE-like morphology during cell culture [12]. Differences in RPE cell proliferation rates have been noted between polyamide nanofibrous scaffolds and traditional substrates like plastic or glass [12].

Electrospinning, a well-established technology, produces ultrathin polymer fibers, including PCL, a biodegradable polyester approved by the FDA for human applications such as drug delivery systems, sutures, and adhesion barriers [13]-[16]. Our primary objective is to bioengineer novel thin 3D nanofibrous membranes using PCL alone and PCL/gelatin combinations (PCL/5% gel, PCL/15% gel, PCL/30% gel) via electrospinning. These nanofibrous networks aim to replicate human BM's structural architecture and function.

Functional analyses of the artificial BMs involved culturing ARPE-19 cells, a human RPE cell line, on 3D nanofibrous membranes to evaluate cellular adhesion, viability, and morphological polarity. Like native RPE cells, ARPE-19 cells express specific genes such as RPE65 and *Zone-Occludens*-1 (ZO-1) and perform phagocytosis of shed rod and cone components [6] [17].

Our findings demonstrate that PCL/30% gelatin serves as a viable scaffold for ARPE-19 cells, promoting cell proliferation, acquiring RPE-like morphology, and maintaining normal expression levels of key RPE cell markers such as RPE65 and ZO-1 after 25 days of culture.

2. Material and Methods

2.1. Bio-Engineering of Ultrathin 3D Nanofibrous Polycaprolactone Membranes

First, we fabricated polycaprolactone-gelatin (PCL-Gel) electrospun nanofibers with different concentrations of Gel (Powder Gelatin Type B; J.T Baker) through electrospinning process was performed in order to create a random 3D nanofibrillar bio-network sharing structural architecture with a functional human BM. Nanofibers were fabricated by solving PCL (medium molecular weight M_n = 80,000, Sigma-Aldrich) in glacial acetic acid (J.T. Baker) at 19 wt/v% and adding to independent solutions the corresponding amount of gelatin to make 5%, 15% and 30% w/w PCL/Gel solutions in acetic acid. Solutions were stirred at 300 rpm during 72 h at RT. Then, electrospinning was carried out using horizontal electrospinning equipment assembled in our laboratory. The electrospinning process was conducted at 17 kV, using a flow rate of 1 mL/h and a collector-ejector distance equal to 18 cm. Finally, all electrospun fibers were collected and cut into 8 mm diameters disks and sterilized by UV light exposition (λ = 254 nm) before cell seeding.

After electrospinning membranes were collected, washed with ethanol and double distilled water (dd-H_2O) and oven-dried (36˚C). These processes were performed in a clean room set up to obtain a clinical grade product. After the fabrication of the fibrils, PCL nanofibrils were chemically cross-linked, cutted, sterilized and dried for 24 hours before them were used in cell cultures. Membranes were named accordingly to their composition PCL/gelatin wt.% in electrospinning solutions.

2.2. Preparation of RPE Cultures

All study protocols adhered to the provisions of the Declaration of Helsinki for research involving human tissue. A commercially available human retinal pigmented epithelium cell line (ARPE-19) from ATCC. Cells were first grown in Dulbecco's modified Eagle's medium (D-MEM) (Thermo Fisher Scientific) with 10% fetal bovine serum (FBS) until confluence. To ensure sterilization, these were initially exposed to ultraviolet (UV) radiation for 1 h in a Biostar cabinet from Telstar S.A. (Madrid, Spain). Thereafter, the cells were passaged by trypsin and seeded onto different fiber scaffolds in 48-well plates at a density of 3×10^4 cells cm in the same media for in vitro experiments, empty wells (without scaffolds) were used as controls (Standard tissue culture polystyrene (TCPS)). Two different cell culture protocols were probed in order to determine which one increase the adhesion of ARPE-19 cells onto the membranes. In the first one, 3×10^4/300 µl cells were seeded onto membranes, in the second one, 3×10^4/30 µl cells were seeded onto membranes, and after 30 minutes medium was added to complete 300 µl. In both protocols DMEM/penicillin-streptomycin 1% and Fetal Bovine Serum (FBS) 10% (supplemented medium) was used. The plates containing the cultured cells on the electrospun membranes were then kept in an

incubator at 5% CO_2, at 37˚C for 24 hours.

2.3. ARPE19 Viability and Proliferation Assays Seeded onto PCL/Gel Membranes

ARPE19 cell cultures were deprived of FBS during 24 hours in order to avoid any participation of FBS components in the following and the 3-(4,5-dimethylthiazol-2-yl)-2,5-diphenyltetrazolium bromide (MTT) experiments. Proliferation and viability assays were performed in reference to the manufacturer's instructions (Cell Proliferation Kit II (MTT proliferation from ROCHE). The LC50 assay was conducted (data not shown), and based on the results, it was determined to work with these three specific concentrations of PCL/gelatin.

The performance of the electrospun membranes was compared to TCPS plate. Three samples from each group of membranes were individually washed and transferred to a new 24-well plate containing 200 µl of DMEM/penicillin-streptomycin for MTT assays in order to measure only the cell viability of the ARPE-19 cells that adhered to the membranes. 50 µl of MTT solution were added to each well. MTT assays were carried out for 45 minutes at 37˚C. Finally, for each well and condition, 100 µl of medium were taken and placed into a new well of a 96-well plate by duplicate. Cell viability, regarding absorbance, was determined by spectroscopy with a microplate reader at 540 nm (Biotek).

A standard curve of ARPE 19 cells, was used as a reference for MTT assays. All assays were individually performed four times. Data were analyzed by one-way ANOVA and Friedman test using GraphPad Prism software (GraphPad Software Inc.), and $p < 0.05$ was regarded as statistically significant with a 95% confidence interval.

2.4. Immunodetection Assays

Immunofluorescence assays were performed to certify the growth and distribution of ARPE-19 cells after 48 h of seeding. First, cells onto membranes were washed three times in PBS1X/Tween 0.02%; then, the membranes were incubated for 1 hour in the same solution for permeabilization. Posteriorly, membranes were incubated in PBS1X/BSA 0.02 for blocking unspecific unions. Then, ARPE-19 cells on different membranes (PCL, PCL/gelatin) were incubated with monoclonal mouse anti-RPE65 antibody (Novus NB-100-355), rabbit anti-actin primary antibodies (1:100 dilution, Santa Cruz Biotechnologies, CA, USA) and rabbit anti-cytokeratin 18 (1:100 dilution, Biorbyt Ltd. Cambridge, UK), overnight at 4˚C. Then, cells were rewashed three times using PBS1X /Tween 0.02%. Posteriorly, membranes were incubated with secondary antibodies; Alexa fluor goat anti-rabbit 488, Alexa fluor goat anti-rabbit 594 and Alexa-fluor goat anti-mouse 488 (1:200 dilution). After two hours of incubation, the membranes were washed using PBS/tween 0.02% four times during 3 min and mounted using VECTASHIELD Antifade Mounting Media with DAPI (Vector Laboratories). All images were taken at random locations with the confocal microscope Axio Imager M1 fluorescence microscope (Zeiss). In this analysis, comparation

were made using PCL as control.

2.5. ARPE19 Cell Morphology by Scanning Electron Microscopy

Eight-mm diameter disc obtained from different 3D nanofibrous scaffolds were placed in 48-well plates and immersed with the same media for *in vitro* experiments. A density of 3×10^4 ARPE-19 cells was seeded in the central part of each disc, and cultured during 25 d. A standard method for SEM preparation was used [18]. Briefly, specimens, *i.e.*, cells on scaffolds, were fixed with 4% paraformaldehyde/0.5% glutaraldehyde mixture diluted in 0.1M sodium cacodylate buffer (pH 7.2) at 4˚C, overnight. Then, fixative mixture was removed, and specimens were washed carefully three times with 0.2M sodium cacodylate buffer (pH 7.2) at 4˚C, using Pasteur pipettes. Postfixation was carried out with 1% osmium tetroxide in 0.1 M sodium cacodylate buffer (pH 7.4) for 2 h, at 4˚C. Once again, the specimens were washed as mentioned and were then dehydrated with increasingly graded ethanol (30% to absolute ethanol) until propylene oxide, at room temperature. As soon as it was possible, were dried by the Critical Point method in a Samdri 780A desiccator (Rockville, MD, USA) using CO_2. Specimens were mounted on aluminum stubs with silver paste and placed in a high vacuum evaporator for gold coating during 6 min in a metal ionizing JEOL JFC-1100 (Fine Coat® ion Sputter, JEOL Ltd, Tokyo, JP). Finally, specimens were examined with a Zeiss DSM-950 scanning electron microscope (Carl Zeiss, Jena, DE) at 25 kV and a 10 mm working distance. Electron micrographs were recorded (55 P/N film; Polaroid Corp., Cambridge, MA) of each sample at random locations.

2.6. Real-Time Quantitative PCR

To confirm the expression of ARPE19 cells, qRT-PCR assays were performed. Briefly, RNA was isolated from ARPE-19 cells seeded in different scaffolds using the RNA extraction Kit from ZYMO Research as instructed by the manufacturers. The RNA was treated with RQ1-RNase-free DNase (Promega, Southampton, UK) to remove any contaminating DNA. First-strand cDNA synthesis was performed on 3 μg of total RNA, AffinityScript QPCR cDNA Synthesis Kit) at 50˚C, according to the manufacturer's protocol. A reaction containing no reverse transcriptase was also prepared for each RNA sample as a control (-RT). Following cDNA synthesis, all reactions were treated with RNase H (Invitrogen) to degrade the RNA template.

PCR was performed on the first-strand cDNA synthesis reaction products, using the SuperScript III Platinum CellsDirect Two-Step qRT-PCR kit (Invitrogen) according to the manufacturer's protocol with gene-specific primers (synthesized by Instituto Nacional de Biotecnología, UNAM, México). The primers were as follow: RPE65 GCC CAG GAG CAG GAC AAA AGA A FW, RPE65 GCG CAT CTG CAA GTT AAA CCA T REV, ZO-1 FW 5'-TGCCATTACACGGTCCTCTG-3' and ZO-1 REV 5'-GGTTCTGCCTCATCATTTCCTC-3' and GAPDH specific primer pair

(5'-GGAAGGTGAAGGTCGGAGTCA; 5'-CTTCCCGTTCTCAGCCTTGAC) as a reference gene for mRNA.

Duplicate PCR reactions were prepared using 5 µl cDNA with q-PCR (Brilliant II SYBR® Green QRT-PCR Master Mix with ROX, 1-Step) and 0.2 µM of gene-specific primer in a total volume of 20 µl. The RT-PCR reaction was performed on a RotorGen (Qiagen, Fast Real-Time PCR System (Warrington, Cheshire, UK)) according to the manufacturer's instructions. Fluorescence signals produced by binding of SYBR Green to new double-stranded amplicons were collected after each PCR cycle. The manufacturer's default thermal cycling conditions were followed (40 cycles of 1 s at 95˚C and 20 s at 60˚C). Data were analyzed using Rotor gen Software analysis (Applied Biosystems), and raw fluorescence data were exported into the DART–PCR spreadsheet to calculate relative gene expression normalized to the geometric mean of glyceraldehyde-3-phosphate dehydrogenase (*GAPDH*). The specificity of all primers was assessed by gel electrophoresis of amplified products, and examination of the dissociation curve. The relative expression levels of RPE65 and ZO-1 of ARPE-19 cells on each membrane levels were assessed using SigmaStat 3.5 software (Systat Software, Inc., Chicago, IL). The results were expressed as *n*-fold induction or inhibition in gene expression relative to endogenous control calculated using the $\Delta\Delta C_T$ method. Two-tailed Student *t*-tests will be performed to compare expression in each different membrane.

2.7. Statistical Analysis

Triplicate wells were used to calculate proliferation ratios and the final number of ARPE19 cells seeded onto each different membrane. The viability assay of ARPE19 cells on different membranes were analyzed in pairs by one-way analysis of variance (ANOVA) and Friedman tests with SPSS Statistic Software (IBM). Data from all experiments were pooled and expressed as the mean SD. A confidence level of p 0.05 was considered to be statistically significant.

3. Results

3.1. ARPE19 Cell Viability Assays in Different Scaffolds

Cell viability studies were performed by spreading ARPE 19 cells on the here developed membranes. The first assays were performed to evaluate two different procedures for cell culture onto the membranes, and only significant results are presented. Cell viability was increased when cells were seeded in a small volume of DMEM medium (1.5×10^4 cells/100 µl) and allowing the cellular adhesion to membranes for 30 minutes, and the medium was added to complete the total volume of each well (**Figure 1**). In these first results, MTT assays shown that there is a significant increase in optical density (490 nm) in the wells corresponding to PCL/30% gelatin, indicating a significant number of cells added to this membrane compared to PCL, PCL/5% and PCL/15% (Data not shown).

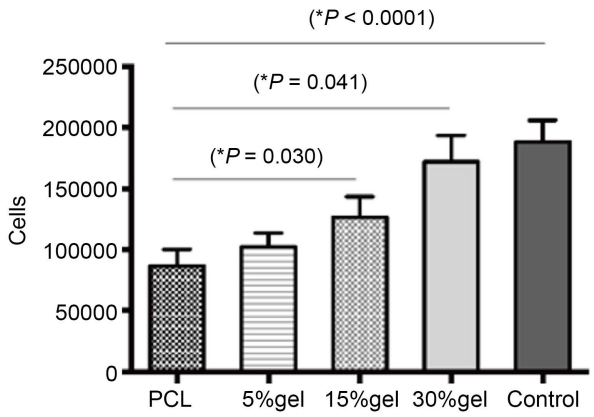

Figure 1. Cell viability of ARPE19 cells cultured onto different membranes. Cell viability of ARPE19 cells cultured onto different types of nanofibrous membranes.; 30,000 ARPE19 cells were resuspended in 300 uL of DMEM medium and carefully seeded in a drop. Cells seeded onto PCL/15% gelatin and PCL/30% gelatin membranes present major viability and the results are statistically significant (*p = 0.030 and *p = 0.041 respectively). ANOVA test was employed to determine statistical significance; and Holm-Sidaks test for multiple comparisons.

However, the degree of cell proliferation and the number of cells expressed as the number of viable cells over the membranes could be obtained when a standard curve of cells was used.

Cells were seeded as we mentioned before, incubated in DMEM medium/10% FBS/1%penicillin-streptomycin 24 hours, FBS deprived 24 hours, and MTT assays were performed. After 30 minutes of incubation in MTT solution, 200ul of each well containing ARPE19 cells successfully attached onto different membranes as well, the standard TCPS plate used as control were analyzed by spectrophotometry using a 96 wells ELISA plate by duplicate. The results showed a significant increase in the number of cells added on the PCL/15% gelatin (*p = 0.030) and PCL/30% gelatin membranes (*p = 0.041) just below the value of the cells seeded on TCPS (control) ($p < 0.0001$) "**Figure 1**".

3.2. Immunodetection of ARPE19 Cells on PCL/30% Gelatin

The MTT assays showed that the membranes constructed in combination with gelatin 30% allow a better cellular adhesion and viability. Considering this fact, the next experiments were performed only onto the PCL/30% combination and compared to PCL as control. In order to observe cell morphology and cytoskeleton of ARPE-19 cells seeded on these membranes, immunofluorescence (IF) assays were performed using antibodies to actin cytoskeleton "**Figure 2**" and cytokeratin18 to observe intermediate filaments "**Figure 3**".

To observe the expression of one of the most used RPE markers (RPE65) IF assays were performed after 25 days of cultured onto PCL and PCL/30%Gel. "**Figure 4**" show an RPE-like morphology and a similar expression pattern to normal human RPE when cells were cultured onto PCL/30% gelatin compared to PCL.

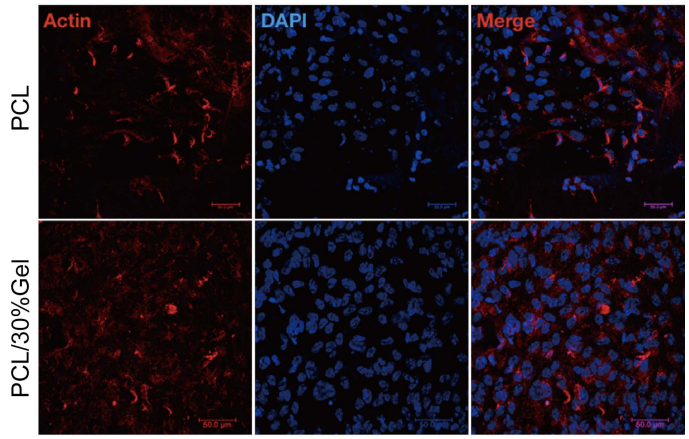

Figure 2. Immunofluorescence assays on 3 × 10^4 ARPE 19-cells seeded onto PCL and PCL/30% gelatin stained with mouse anti-actin, (red) and DAPI to label nuclei (blue). Observe a major number of cells and different arrangement of actin in cells seeded onto PCL/30% Gelatin.

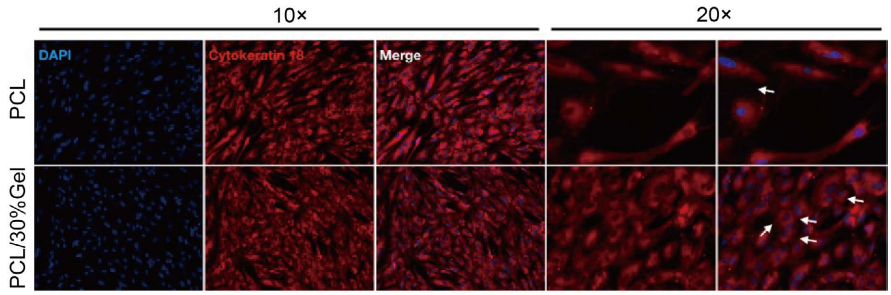

Figure 3. Immunofluorescence assays on 3 × 10^4 ARPE 19-cells seeded onto PCL and PCL/30% gelatin stained with mouse anti-cytokeratin 18 (red) and DAPI to label nuclei (blue). Observe a major number of cells and different arrangement of cytokeratin as well as the more hexagonal morphology in cells seeded onto PCL/30% Gelatin (white arrows).

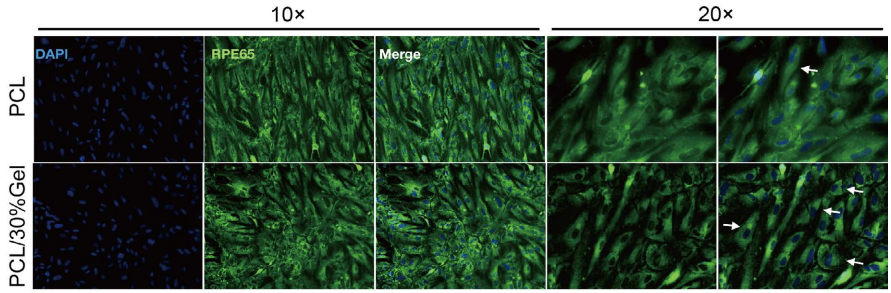

Figure 4. Immunofluorescence assays on 3 × 10^4 ARPE 19-cells seeded onto PCL and PCL/30% gelatin stained with mouse anti-RPE65 (green) and DAPI to label nuclei (blue). Observe a major number of cells and different arrangement of RPE65 as well as the more hexagonal morphology in cells seeded onto PCL/30%Gelatin (white arrows).

3.3. Structural Characteristics of Membranes

Figure 5 shows the SEM images of the electrospun membranes for PCL and PCL/30%Gelatin. As it can be observed in **Figure 5(A)**, **Figure 5(B)**, **Figure 5(D)**, **Figure 5(E)** the neat of PCL/30%Gelatin solution resulted in uniform ul-

trathin fibers (red arrows). These fibers exhibited differences in its nanofibrillar structure than the PCL gelatin membranes (F), probably due to the effect of the addition of gelatin.

As it can be seen in Figure 5, as a result of the culture conditions the PCL membrane partially lost its fiber-based morphology after 25 days in culture. Interestingly, it resulted in a more continuous structure showing a reduction of its fibrillar characteristics. Figures 5(A)-(C) shows the ARPE-19 cells onto the PCL/30%Gelatine membrane. As we can see, these cells exhibit an RPE-like epithelial morphology, densely packed and present hexagonal shape (green arrows) and apical microvilli (white arrows in C).

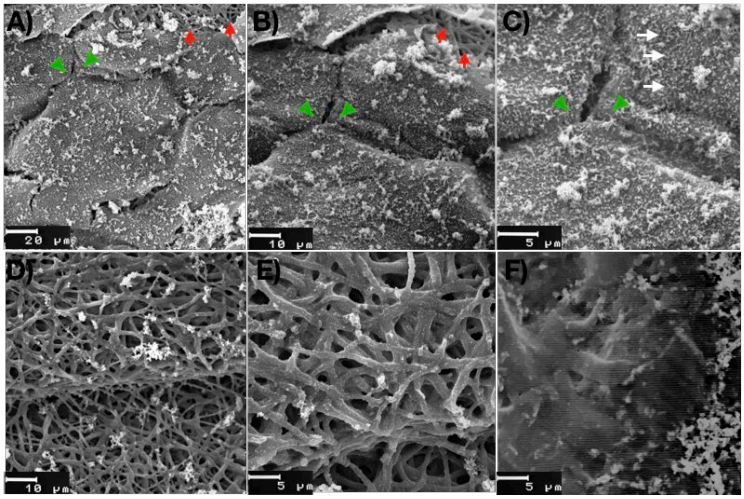

Figure 5. Scanning electron microscopy (SEM) of ARPE-19 cells after 25 days in culture onto 3D nanofibribous membranes of poly-(ε-caprolactone) (PCL/30% gelatine), bio-engineered through electrospinning process. The ARPE-19 cells formed a monolayer of polygonal cells on the PCL/30% gelatine scaffold (A, B, C) but not when were cultured onto PCL membranes (F). Apical surfaces of ARPE-19 cells showed a rough and furry aspect due to the presence of abundant and very small protrusions of the membrane (C, white arrows). This was not observed in the very scarce cells ARPE-19 cells adhered to PCL membranes (F). Note the presence of very narrow adhesion zones among the contours of the polygonal cells of the monolayer (A, B, C, green arrowheads). Some areas of detached cell monolayer, probably in an artefactual way, allowed to observe the 3D nanofibrous membranes of PCL/30% (A, B, red arrowheads). The 3D structure of these nanofibrous scaffolds are better observed in regions without adhered ARPE-19 cells (D, E).

3.4. Expression of RPE Markers

To address quantitative changes in gene expression of both principal markers of RPE cells, we used qRT-PCR to evaluate expression changes of RPE65 and ZO-1 on ARPE19 cells cultured for 25 days. As we can observe in Figure 6, there are non-significant changes in the expression of these markers. There is a slight fold increase on the expression of RPE65 and ZO-1 in cells seeded in PCL/30% gelatin membranes. However, as we mentioned before, is not statistically significant. Suggesting that these membranes do not affect the expression patterns of ARPE19 cells seeded and cultured on the membranes produced.

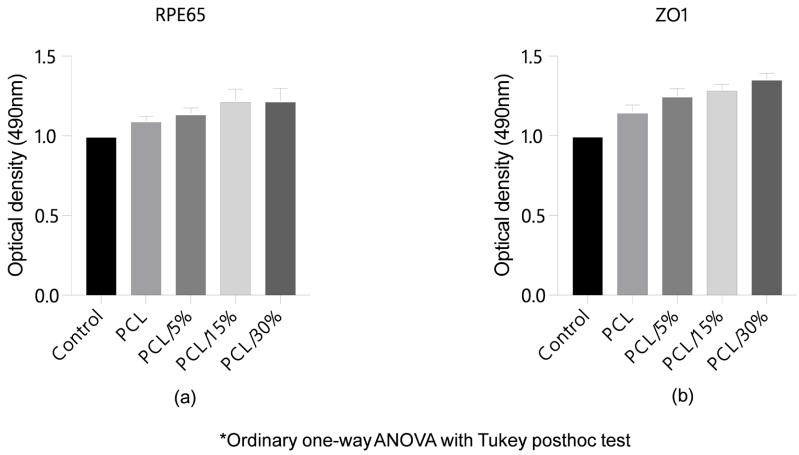

Figure 6. Real-time PCR analysis of RPE markers RPE65 and ZO-1 in ARPE-19 cells seeded onto PCL, PCL/5%Gel, PCL/15%Gel, and PCL/30%Gel showing that there were no statistical differences in the expression of both RPE65 (a) and ZO-1 (b) in cells seeded onto the different membranes. A slight tendency to increase expression of both markers is observed. The bar graph shows the normalized expression folds in RPE cells cultured onto different membranes. Data are the mean SE of four independent experiments. $p > 0.05$ by ANOVA with posthoc test.

4. Discussion

To Retinal degenerative diseases such as AMD, Stargardt's disease (SD) Macular hole, Diabetic retinopathy (DR) and Retinitis pigmentosa (RP) are the leading causes of blindness worldwide. There are some treatments like anti-angiogenic drugs, laser photocoagulation or RPE cell replacement therapy [3] [18]. However, there is no an effective therapy to stop the progression and more importantly, to restore the lost vision on these ocular pathologies.

The use of anti-angiogenic therapies for the "wet" form of AMD have shown the reduction of choroidal neovascularization with intraretinal or subretinal leakage, as well as, the reduction of hemorrhages, and RPE detachments after long periods of treatment. In reality, these therapies are not modifying the progression of these pathologies, only helps to delay it [19]. Regarding RPE cell replacement option, it is an excellent idea since it is directed to replace and restore the RPE and it has been performed in animal models and human patients of AMD [3] [20]-[22]. Nevertheless, these therapies are far from being perfect, and there is still ample room for improvement.

In another way, there is a vast number of scientific reports showing advances in the design, construction, and functionality of a BM for RPE reconstruction in order to restore vision in different ocular pathologies, such as AMD. [3] [18] [23]-[25]. Despite these advances, there is a lack of a functional BM capable of supporting and restoring RPE. An artificial and functional BM have to present a similar BM natural ultrastructure, resistance to biodegradability and support RPE cells in cultures.

In this study, we used PCL and a combination of PCL and different concentrations of Gelatine (5%, 15%, 30%) as possible biological support for ARPE-19

cell culture since it can be acquired more efficiently than any other synthetic substrates.

First, when ARPE-19 cells (3×10^4) were seeded in a small volume (30 µl) the cellular viability was increased compared to cells seeded in 300 µl onto these membranes (**Figure 1(A)**), we suggest that this result was a consequence of having allowed the cells to adhere to the membranes for 30 minutes before to complete the total volume of medium. This procedure was performed on the other set of experiments.

When a standard curve of cells was used as a reference in order to obtain a more precise number of seeded cells onto the different membranes, the results show a significant increase of ARPE-19 cells onto the PCL/15%Gel and PCL/30%Gel membranes. For instance, both membranes allowed proliferation of these cells until MTT assay were performed.

There is a previous report using PCL/gelatin/Ketoprofen combination. However, the authors only used one more diluted concentration of gelatine in its preparation and as we have mentioned before, Ketoprofen (a non-steroidal anti-inflammatory drug [13]. They have fabricated this combination as a drug delivery system and when they seeded cells onto its membrane, cells highly proliferated and certain cells overgrowth and show agglomeration [13]. Shadforth *et al*., used *Bombix mori* silk fibroin (BMSF) as a mat for human RPE cells. They show that BMSF in combination with ECM proteins (laminin, fibronectin, and vitronectin) increase the cell attachment in long-term cultures of ARPE-19 and primary cultures of human RPE cells [26]. However, their results shown a slower growth of human RPE cells seeded onto vitronectin-coated-MBSF [26]. In our results, there is no an agglomeration of ARPE-19 cells, and MTT assays did not show any reduction on cellular proliferation when compare to the number of cells seeded directly on TCPS wells (control). The control TCPS presented a slightly higher number of cells-attached. This effect is probably due to the capabilities of the samples to retain the contact between the liquid phase and a solid surface (wettability). It is well known that highly hydrophobic polymers, such as PCL tend to exhibit relatively poor cell attachment performance [16] [23]. Interestingly, as we said before, the PCL/30%Gel membrane showed a similar attachment performance, in comparison of both TCPS and better performance compared to the PCL membrane. This observation could be due to the hydrophilic nature of gelatin as well as the high porosity of the fibers showed in this combination. In this part, we can conclude that membranes of PCL/30%Gelatine, without any other factor or compound added, are an excellent option to ARPE-19 support.

In addition, to support ARPE-19 or RPE attachment, our membrane or any material to be used as scaffold for RPE must support and allow a fully differentiated RPE monolayer. Among the principal characteristics of a well differentiated and functional RPE is the tightly hexagonal morphology, that can be observed using some RPE markers such as ZO-1, RPE65, or the peripheral distribution of F-actin fibers and cytokeratin 18 [26]-[29].

We performed IF assays to observe actin and cytokeratin distribution, as well as RPE65 in ARPE-cells, seeded in PCL and PCL/30%Gelatin. The results show differences on actin and cytokeratin distribution. In ARPE-19 cells on PCL, we observe a more centralized distribution and more stress fibers. However, actin on ARPE-19 cells seeded onto PCL/30%Gelatine exhibit a reduction in stress fibers and a more peripheral arrangement of actin as well as cytokeratin 18.

These results are like previous reports, where the analysis of F-actin shown a similar distribution patterns in long term RPE cells cultures grown on BMSF [30]. It has been demonstrated that low-phagocytic RPE cells possess an abnormal F-actin distribution in RPE cells, characterized by the lack of peripheral and circumferential F-actin, less apical F-actin and the presence of stress fibers [30]. Our results show that there is a tendency to a re-arrangement of actin and cytokeratin to the cell periphery, and suggest that ARPE-19 cells are recovering their normal phagocytic activities. However, more studies are needed in order to prove it.

Regarding to the arrangement of cytokeratin18, we observe similar differences between the pattern observed in ARPE-19 cells on PCL and PCL/30%Gelatin. It has been demonstrated that a continued Cytokeratin 18 expression could help to preserve RPE epithelial phenotype in long term cultures [25] [31]-[34]. Using both cytoskeleton markers, we can observe the deposition of ARPE-19 cells onto the membranes. However, when cells were seeded onto PCL/30% membrane, its cytoskeleton distribution exhibited a more tightly formed RPE monolayers with characteristic polygonal RPE-like cell structures suggesting a more functional ARPE-19 cell. Finally, no significant differences appeared between PCL and PCL/30%Gelatin membranes with respect to the intracellular localization of RPE65 protein by IF. However, our results show that cells seeded onto PCL%30Gelatin exhibit different morphological characteristics. These cells presented a marked polygonal morphology when compared to PCL suggesting that there is a tendency to a healthy, mature and more differentiated RPE monolayer. Related to this, we performed qRT-PCR assays to evaluate if these slight differences on ARPE-19 morphology were related to changes in gene expression of RPE markers; RPE65 and ZO-1. Although no statistically significant increased expression was observed for RPE65 and ZO-1 in cells seeded on any membrane (PCL, PCL/5%Gelatin, PCL/15%Gelatin and PCL/30%Gelatin), there was a slight tendency to increase the expression of both markers suggesting that our membranes did not disturb normal RPE-cell gene expression. Some authors have suggested that the increased expression and maintenance of RPE genes such as RPE65 and ZO-1 over long-term culture, suggests that RPE cells are attached, proliferating and forming functional monolayers on different scaffolds like our PCL/30%Gelatin [34]-[37]. Although no significant changes in the expression of these genes were observed, qRT-PCR analysis showed a ~0.25 increase fold in the of both markers. This is a remarkable finding because it has been demonstrated that RPE65 deficiency led to alterations in mammalian vision and failures in the retinoid cycle producing human blindness and the increase of RPE expression drives to the

differentiation of Human Stem Cells to RPE phetnotype [35].

These ARPE-19 cells express the tight junction complex protein ZO-1 without significant changes. ZO-1 is a junctional adaptor protein that interacts with multiple other junctional components, including the transmembrane proteins of the claudin and JAM families. It has been proved that ZO-1 depletion leads to selective loss of tight junction proteins, loss of barrier formation and loss mechanotransducers such as vinculin and PAK2, inducing vinculin dissociation and finally ARPE-19 cells has been associated with Epithelial-Mesenchymal Transition (EMT) [36] [37]. In another way, when ZO-1 expression is increased, there is a correlation with the acquired epithelial morphology characteristics of the native RPE cells [38] [39]. As a conclusion of this analysis, we observe that our cells do not reduce its RPE65 and ZO-1 normal expression suggesting the presence of healthy ARPE-19 cells on our membranes.

Finally, the ARPE-19 cells seeded as well as the constructed membranes using PCL/30%Gelatin showed a more "natural appearance" compared to PCL and other membrane-like scaffolds previous reported [40]-[42]. When we observe our PCL/30/Gelatin, we can see a fibrillar network supporting differentiated ARPE-19 cells. The membrane made only by PCL did not exhibit characteristics such as fibrillar network and ARPE-19 cells. The observed changes in the electrospun PCL/30%Gelatin membrane can be related to the electrospinnability of gelatin from the acetic acid solution, affecting parameters like polymer degradation [42]. Contrary to what was expected, PCL/30%Gelatin membranes retained their fibrillar characteristics and exhibited a porous membrane make them permeable to nutrient exchange regulated by BM. Besides, the surface topography and nanofiber arrangement observed in these membranes could increase the impact on cell functions, cellular adhesion and maturation positively influencing RPE cell attachment and monolayer formation.

In spite of we used ARPE-19 cells in these experiments, this cell line has been broadly used as an alternative to human RPE as these cells present epithelial cell morphology and specific markers of RPE such as RPE65 (abundantly expressed in the RPE); cellular retinaldehyde-binding protein (CRALBP), a retinoid-binding protein involved in the regeneration of visual pigment. Finally, these cells perform assimilation of outer photoreceptor segments (POS) by phagocytosis [6] [43] [44]. The use of this cell line allows us to demonstrate that membranes composed by PCL/30%Gelatin are an excellent option as a scaffold to grow, support and differentiate ARPE-19 cells and possibly human RPE cells. As Xiang *et al*. has mentioned [18], the ideal artificial BM would exhibit properties such as: thickness of less than 5 mm; a porous ultrastructure; biocompatibility for cell adhesion and growth; no expression changes in genes of RPE, preserve the physiological RPE features like polygonal shape and formation of tight junctions, phagocytosis of ROS, formation of apical microvilli, the polarized secretion of neurotrophic factors, and without inflammation after implantation. Our results show that these membranes exhibit some of the ideal BM characteristics for subretinal implantation in patients with wet age-related macular degenera-

tion (AMD) where there is a rupture of the Bruch's membrane caused by the growth of blood vessels. However, longer-term investigation and *in vivo* studies need to be carried out to prove it.

5. Conclusions

1) We have shown that our fabricated PCL/30%Gel nanofibrous membranes provide a micro-architecture mimicking the inner collagenous layer of the human BM.

2) We demonstrated the superiority of our PCL/30%Gel nanofibrous membrane in their ability to provide an artificial niche for ARPE19 cells which allowed such cells to maintain their bio functionality and morphological characteristics of RPE that additionally presents improved cross-linking characteristics similar to natural human Bruch's membrane.

3) The nanofibrous membranes can be fabricated repeatedly and could be surgically handy.

4) For our knowledge, no previous studies are showing these results on these kinds of membranes.

5) Finally, it could be used posteriorly in translational medicine for AMD patients.

Acknowledgements

We gratefully acknowledge support from generous benefactors of the Asociación Para Evitar la Ceguera en México, a non-profit organization for funding this research. Special thanks to Biologist Armando Zepeda Rodríguez for technical assistance on SEM microscopy (Departamento de Biología Celular y Tisular, School of Medicine-UNAM) and Dr. José Luna Muñoz for confocal microscopy assistance.

Competing Interest

All authors certify that they have NO affiliations with or involvement in any organization or entity with any financial interest, or non-financial interest in the subject matter or materials discussed in this manuscript.

References

[1] Curcio, C.A. and Johnson, M. (2012) Structure, Function, and Pathology of Bruch's Membrane. *Retina Fifth Edition*, **1**, 465-481.

[2] Smith, W., Assink, J., Klein, R., Mitchell, P., Klaver, C.C.W., Klein, B.E.K., *et al.* (2001) Risk Factors for Age-Related Macular Degeneration. *Ophthalmology*, **108**, 697-704. https://doi.org/10.1016/s0161-6420(00)00580-7

[3] Hernández-Zimbrón, L.F., Zamora-Alvarado, R., Ochoa-De la Paz, L., Velez-Montoya, R., Zenteno, E., Gulias-Cañizo, R., *et al.* (2018) Age-related Macular Degeneration: New Paradigms for Treatment and Management of AMD. *Oxidative Medicine and Cellular Longevity*, **2018**, 1-14. https://doi.org/10.1155/2018/8374647

[4] Velez-Montoya, R., Oliver, S.C.N., Olson, J.L., Fine, S.L., Mandava, N. and Qui-

roz-Mercado, H. (2013) Current Knowledge and Trends in Age-Related Macular Degeneration. *Retina*, **33**, 1487-1502. https://doi.org/10.1097/iae.0b013e318271f265

[5] Salvi, S.M., Akhtar, S. and Currie, Z. (2006) Ageing Changes in the Eye. *Postgraduate Medical Journal*, **82**, 581-587. https://doi.org/10.1136/pgmj.2005.040857

[6] William, S., *et al*. (2017) Appropriately Differentiated ARPE-19 Cells Regain Phenotype and Gene Expression Profiles Similar to Those of Native RPE Cells. *Molecular Vision*, **23**, 60-89. http://www.molvis.org/molvis/v23/60

[7] Bhutto, I. and Lutty, G. (2012) Understanding Age-Related Macular Degeneration (AMD): Relationships between the Photoreceptor/Retinal Pigment Epithelium/Bruch's Membrane/Choriocapillaris Complex. *Molecular Aspects of Medicine*, **33**, 295-317. https://doi.org/10.1016/j.mam.2012.04.005

[8] Binder, S., Stanzel, B.V., Krebs, I. and Glittenberg, C. (2007) Transplantation of the RPE in AMD. *Progress in Retinal and Eye Research*, **26**, 516-554. https://doi.org/10.1016/j.preteyeres.2007.02.002

[9] Warnke, P.H., Alamein, M., Skabo, S., Stephens, S., Bourke, R., Heiner, P., *et al*. (2013) Primordium of an Artificial Bruch's Membrane Made of Nanofibers for Engineering of Retinal Pigment Epithelium Cell Monolayers. *Acta Biomaterialia*, **9**, 9414-9422. https://doi.org/10.1016/j.actbio.2013.07.029

[10] Surrao, D.C., Greferath, U., Chau, Y., Skabo, S.J., Huynh, M., Shelat, K.J., *et al*. (2017) Design, Development and Characterization of Synthetic Bruch's Membranes. *Acta Biomaterialia*, **64**, 357-376. https://doi.org/10.1016/j.actbio.2017.09.032

[11] Burkersroda, F.v., Schedl, L. and Göpferich, A. (2002) Why Degradable Polymers Undergo Surface Erosion or Bulk Erosion. *Biomaterials*, **23**, 4221-4231. https://doi.org/10.1016/s0142-9612(02)00170-9

[12] Thieltges, F., Stanzel, B.V., Liu, Z. and Holz, F.G. (2011) A Nanofibrillar Surface Promotes Superior Growth Characteristics in Cultured Human Retinal Pigment Epithelium. *Ophthalmic Research*, **46**, 133-140. https://doi.org/10.1159/000324045

[13] Basar, A.O., Castro, S., Torres-Giner, S., Lagaron, J.M. and Turkoglu Sasmazel, H. (2017) Novel Poly(ε-Caprolactone)/Gelatin Wound Dressings Prepared by Emulsion Electrospinning with Controlled Release Capacity of Ketoprofen Anti-Inflammatory Drug. *Materials Science and Engineering*: *C*, **81**, 459-468. https://doi.org/10.1016/j.msec.2017.08.025

[14] Li, D. and Xia, Y. (2004) Electrospinning of Nanofibers: Reinventing the Wheel? *Advanced Materials*, **16**, 1151-1170. https://doi.org/10.1002/adma.200400719

[15] Prado-Prone, G., Silva-Bermudez, P., Almaguer-Flores, A., García-Macedo, J.A., García, V.I., Rodil, S.E., *et al*. (2018) Enhanced Antibacterial Nanocomposite Mats by Coaxial Electrospinning of Polycaprolactone Fibers Loaded with Zn-Based Nanoparticles. *Nanomedicine*: *Nanotechnology*, *Biology and Medicine*, **14**, 1695-1706. https://doi.org/10.1016/j.nano.2018.04.005

[16] Bahareh, A.*et al*. (2014) Poly (ε-Caprolactone) Fiber: An Overview. *Journal of Engineered Fibers and Fabrics*, **9**, 74-90. https://journals.sagepub.com/doi/pdf/10.1177/155892501400900309

[17] Alizadeh, Mitra, *et al*. "Downregulation of differentiation specific gene expression by oxidative stress in ARPE-19 cells." *Investigative ophthalmology & visual science* 42.11 (2001): 2706-2713. http://intl.iovs.org/cgi/content/abstract/42/11/2706

[18] Xiang, P., Wu, K., Zhu, Y., Xiang, L., Li, C., Chen, D., *et al*. (2014) A Novel Bruch's Membrane-Mimetic Electrospun Substrate Scaffold for Human Retinal Pigment Epithelium Cells. *Biomaterials*, **35**, 9777-9788.

https://doi.org/10.1016/j.biomaterials.2014.08.040

[19] Velez-Montoya, R., Oliver, S.C.N., Olson, J.L., Fine, S.L., Quiroz-Mercado, H. and Mandava, N. (2014) Current Knowledge and Trends in Age-Related Macular Degeneration. *Retina*, **34**, 423-441. https://doi.org/10.1097/iae.0000000000000036

[20] Engelhardt, M., Tosha, C., Lopes, V.S., Chen, B., Nguyen, L., Nusinowitz, S., *et al.* (2012) Functional and Morphological Analysis of the Subretinal Injection of Retinal Pigment Epithelium Cells. *Visual Neuroscience*, **29**, 83-93. https://doi.org/10.1017/s0952523812000041

[21] Tezel, T.H., Del Priore, L.V., Berger, A.S. and Kaplan, H.J. (2007) Adult Retinal Pigment Epithelial Transplantation in Exudative Age-Related Macular Degeneration. *American Journal of Ophthalmology*, **143**, 584-595.E2. https://doi.org/10.1016/j.ajo.2006.12.007

[22] Liu, Y., Xu, H.W., Wang, L., Li, S.Y., Zhao, C.J., Hao, J., *et al.* (2018) Human Embryonic Stem Cell-Derived Retinal Pigment Epithelium Transplants as a Potential Treatment for Wet Age-Related Macular Degeneration. *Cell Discovery*, **4**, Article No. 50. https://doi.org/10.1038/s41421-018-0053-y

[23] Hotaling, N.A., Khristov, V., Wan, Q., Sharma, R., Jha, B.S., Lotfi, M., *et al.* (2016) Nanofiber Scaffold-Based Tissue-Engineered Retinal Pigment Epithelium to Treat Degenerative Eye Diseases. *Journal of Ocular Pharmacology and Therapeutics*, **32**, 272-285. https://doi.org/10.1089/jop.2015.0157

[24] Jha, B.S. and Bharti, K. (2015) Regenerating Retinal Pigment Epithelial Cells to Cure Blindness: A Road towards Personalized Artificial Tissue. *Current Stem Cell Reports*, **1**, 79-91. https://doi.org/10.1007/s40778-015-0014-4

[25] Liao, J., Yu, J., Huang, K., Hu, J., Diemer, T., Ma, Z., *et al.* (2010) Molecular Signature of Primary Retinal Pigment Epithelium and Stem-Cell-Derived RPE Cells. *Human Molecular Genetics*, **19**, 4229-4238. https://doi.org/10.1093/hmg/ddq341

[26] Shadforth, A.M.A., George, K.A., Kwan, A.S., Chirila, T.V. and Harkin, D.G. (2012) The Cultivation of Human Retinal Pigment Epithelial Cells on Bombyx Mori Silk Fibroin. *Biomaterials*, **33**, 4110-4117. https://doi.org/10.1016/j.biomaterials.2012.02.040

[27] Bazzoni, G., Martínez-Estrada, O.M., Orsenigo, F., Cordenonsi, M., Citi, S. and Dejana, E. (2000) Interaction of Junctional Adhesion Molecule with the Tight Junction Components ZO-1, Cingulin, and Occludin. *Journal of Biological Chemistry*, **275**, 20520-20526. https://doi.org/10.1074/jbc.m905251199

[28] Fanning, A.S. and Anderson, J.M. (2009) Zonula Occludens-1 and -2 Are Cytosolic Scaffolds That Regulate the Assembly of Cellular Junctions. *Annals of the New York Academy of Sciences*, **1165**, 113-120. https://doi.org/10.1111/j.1749-6632.2009.04440.x

[29] Tornavaca, O., Chia, M., Dufton, N., Almagro, L.O., Conway, D.E., Randi, A.M., *et al.* (2015) ZO-1 Controls Endothelial Adherens Junctions, Cell-Cell Tension, Angiogenesis, and Barrier Formation. *Journal of Cell Biology*, **208**, 821-838. https://doi.org/10.1083/jcb.201404140

[30] Müller, C., Charniga, C., Temple, S. and Finnemann, S.C. (2018) Quantified F-Actin Morphology Is Predictive of Phagocytic Capacity of Stem Cell-Derived Retinal Pigment Epithelium. *Stem Cell Reports*, **10**, 1075-1087. https://doi.org/10.1016/j.stemcr.2018.01.017

[31] Fuchs, U., T. Kivelä, and A. Tarkkanen. (1991) Cytoskeleton in Normal and Reactive Human Retinal Pigment Epithelial Cells. *Investigative Ophthalmology & Visual*

Science, **32**, 3178-3186.
https://iovs.arvojournals.org/article.aspx?articleid=2160461

[32] Chen, J., Dong, R., Ge, J., Guo, B. and Ma, P.X. (2015) Biocompatible, Biodegradable, and Electroactive Polyurethane-Urea Elastomers with Tunable Hydrophilicity for Skeletal Muscle Tissue Engineering. *ACS Applied Materials & Interfaces*, **7**, 28273-28285. https://doi.org/10.1021/acsami.5b10829

[33] Kim, J., Kim, H.N., Lang, Y. and Pandit, A. (2014) Biologically Inspired Micro- and Nanoengineering Systems for Functional and Complex Tissues. *Tissue Engineering Part A*, **20**, 2127-2130. https://doi.org/10.1089/ten.tea.2013.0707

[34] Priore, L.V.D., Geng, L., Tezel, T.H. and Kaplan, H.J. (2002) Extracellular Matrix Ligands Promote RPE Attachment to Inner Bruch's Membrane. *Current Eye Research*, **25**, 79-89. https://doi.org/10.1076/ceyr.25.2.79.10158

[35] Sengupta, N., *et al*. (2006) RPE65 Transgene Induces Bone Marrow Stem Cells to Rescue Retinal Pigment Epithelium Damage. *Investigative Ophthalmology & Visual Science*, 47, Article 1767.
https://iovs.arvojournals.org/article.aspx?articleid=2391630

[36] Lee, J., Ko, M. and Joo, C. (2008) Rho Plays a Key Role in TGF-β1-Induced Cytoskeletal Rearrangement in Human Retinal Pigment Epithelium. *Journal of Cellular Physiology*, **216**, 520-526. https://doi.org/10.1002/jcp.21424

[37] Li, H., Wang, H., Wang, F., Gu, Q. and Xu, X. (2011) Snail Involves in the Transforming Growth Factor B1-Mediated Epithelial-Mesenchymal Transition of Retinal Pigment Epithelial Cells. *PLOS ONE*, **6**, e23322.
https://doi.org/10.1371/journal.pone.0023322

[38] Rizzolo, L.J. (2007) Development and Role of Tight Junctions in the Retinal Pigment Epithelium. *International Review of Cytology*, **258**, 195-234.
https://doi.org/10.1016/s0074-7696(07)58004-6

[39] Georgiadis, A., Tschernutter, M., Bainbridge, J.W.B., Balaggan, K.S., Mowat, F., West, E.L., *et al*. (2010) The Tight Junction Associated Signalling Proteins ZO-1 and ZONAB Regulate Retinal Pigment Epithelium Homeostasis in Mice. *PLOS ONE*, **5**, e15730. https://doi.org/10.1371/journal.pone.0015730

[40] Lavik, E.B., Klassen, H., Warfvinge, K., Langer, R. and Young, M.J. (2005) Fabrication of Degradable Polymer Scaffolds to Direct the Integration and Differentiation of Retinal Progenitors. *Biomaterials*, **26**, 3187-3196.
https://doi.org/10.1016/j.biomaterials.2004.08.022

[41] Tomita, M., Lavik, E., Klassen, H., Zahir, T., Langer, R. and Young, M.J. (2005) Biodegradable Polymer Composite Grafts Promote the Survival and Differentiation of Retinal Progenitor Cells. *Stem Cells*, **23**, 1579-1588.
https://doi.org/10.1634/stemcells.2005-0111

[42] Hu, J., Prabhakaran, M.P., Tian, L., Ding, X. and Ramakrishna, S. (2015) Drug-Loaded Emulsion Electrospun Nanofibers: Characterization, Drug Release and *in Vitro* Biocompatibility. *RSC Advances*, **5**, 100256-100267.
https://doi.org/10.1039/c5ra18535a

[43] Dunn, K.C., Aotaki-Keen, A.E., Putkey, F.R. And Hjelmeland, L.M. (1996) ARPE-19, a Human Retinal Pigment Epithelial Cell Line with Differentiated Properties. *Experimental Eye Research*, **62**, 155-170.
https://doi.org/10.1006/exer.1996.0020

[44] Hamel, C.P., Tsilou, E., Pfeffer, B.A., Hooks, J.J., Detrick, B. and Redmond, T.M. (1993) Molecular Cloning and Expression of RPE65, a Novel Retinal Pigment Epi-

thelium-Specific Microsomal Protein That Is Post-Transcriptionally Regulated *in Vitro*. *Journal of Biological Chemistry*, **268**, 15751-15757.
https://doi.org/10.1016/s0021-9258(18)82319-5